

Resonant optical control of the electrically-induced spin polarization by periodic excitation

F. G. G. Hernandez,^{1,*} G. M. Gusev,¹ and A. K. Bakarov²

¹*Instituto de Física, Universidade de São Paulo, Caixa Postal 66318 - CEP 05315-970, São Paulo, SP, Brazil*

²*Institute of Semiconductor Physics, Novosibirsk 630090, Russia*

(Dated: March 28, 2014)

The electrical and optical spin control methods were combined and implemented in a two-dimensional electron gas. We show that the electron spin polarization generated by an electrical current may have its direction controlled and magnitude amplified by periodic optical excitation. The resulting spin dynamics in an external transverse magnetic field was optically probed using Kerr rotation. We found long spin lifetime for a large range of applied voltage, and strong dependence on the pulse optical power and sample temperature. The signal was mapped in a Hall bar as function of the position relative to the injection contact. Finally, the in-plane current-induced spin polarization was directly measured by rotating the external magnetic field and the internal magnetic field role was analyzed.

Semiconductor quantum wells are largely explored platforms for the future development of spintronic devices using optical and electrical spin control methods [1]. Among the optical techniques using periodical excitation [2], the resonance between the pulse temporal train structure and the spin precession around an external magnetic field (B_{ext}) leads to remarkable phenomena as the resonant spin amplification (RSA) [3] and the mode-locking (ML) effect [4, 5]. At a fixed time delay (Δt) between a circularly polarized pump and a linearly polarized probe, the amplification of the optically generated out-of-plane component occurs when B_{ext} obeys the periodic resonance condition: $\Delta B_{ext} = (hf_1)/(g\mu_B)$ where f_1 is the laser repetition rate. Figure 1(a) shows the RSA geometry where the Kerr rotation angle (ϕ_K) is detected at the pump modulation frequency (f_p). Such synchronization revealed rich spin dynamics for n- and p-doped low-dimensional systems [6] including anisotropic spin relaxation [7, 8], long-lived spin coherence for electrons and holes in quantum wells [9–11] and quantum dots [12–14], as well as interdependent electron and hole spin dynamics [15].

On the other side, electrical generation of spin polarization opens a possibility to develop spin current sources [16, 17] added to the tuning capability of the spin-orbit interaction (SOI) [18, 19]. Two components have been observed in two-dimensional electron gases (2DEG): an homogeneous in-plane current-induced spin polarization (CISP) [20], and an out-of-plane spin polarization accumulated close to the current channel edges resulting from the spin Hall effect (SHE) [20, 21]. The CISP in-plane orientation is determined along the internal magnetic field (B_{in}) which is tunable by an external electric field (E) and perpendicular to its direction. Figure 1(b) displays the continuous-wave configuration for the optical measurement of the CISP precession around B_{ext} where ϕ_K is now detected at the applied voltage frequency (f_2).

In a combination of optical and electrical techniques,

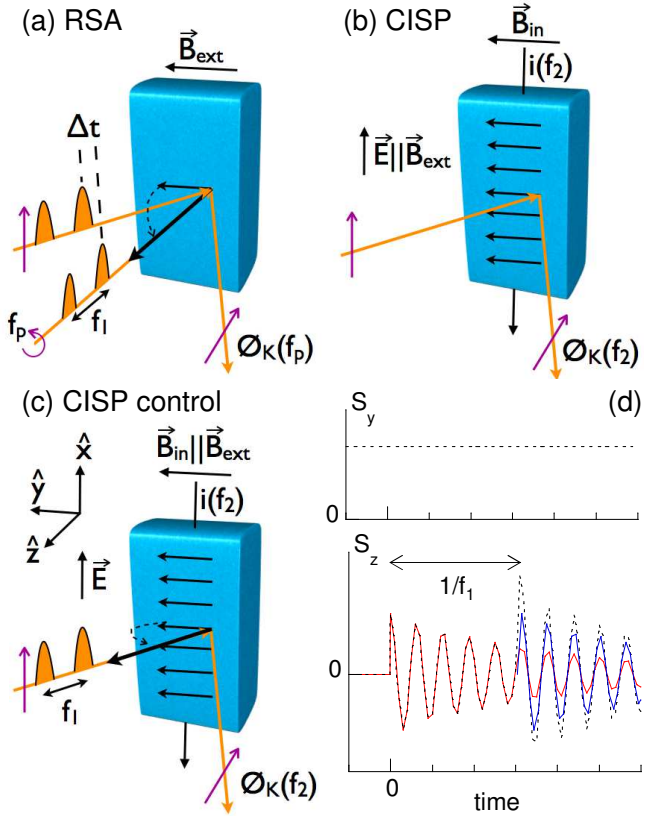


FIG. 1: (Color online) (a) Resonant spin amplification. (b) Optical detection of the CISP. (c) Optical control of the CISP. (d) Components of the spin polarization in (c).

the application of an external electric field on optically generated spin packets showed coherent spin manipulation by the creation of an internal magnetic field [22, 23]. More recently, the electric field reorientation of also optically generated spins was demonstrated [24]. Nevertheless, the opposite situation where a CISP signal is controlled by an optical pulse has not been reported.

Here, we address the amplification and reorientation of the CISP by periodic optical excitation in resonance with a variable external magnetic field. The experimental geometry is shown in Figure 1(c). The CISP was optically probed using Kerr rotation (KR). A mode-locked Ti:sapphire laser was used emitting pulses with 100 fs duration at a rate of 76 MHz. The probe laser was linearly polarized and tuned to the absorption edge of the QW sample with adjustable power. The probe beam polarization and amplitude were not modulated and it was detected by coupled photodiodes. The sample was processed in a Hall bar geometry with ohmic contacts for electrical current injection. In order to detect the spin polarization that arises from the electrical pumping, a sine voltage wave with tunable amplitude and fixed frequency of 1.1402 kHz was used for lock-in detection. The sample was immersed in the variable temperature insert of a superconductor magnet in the Voigt geometry with the current channel perpendicular or along B_{ext} . We explored the manipulation of the spin polarization in a 2DEG by the applied electrical voltage, optical pulse power, and the signal amplitude dependence on the temperature and device geometry. The experimental data displays a RSA pattern with long-lived spin coherence oscillations where the spin lifetime is independent of the current level and strongly damped by high optical power and temperature.

The studied sample is a 45 nm wide GaAs quantum well containing a 2DEG with high electron density $n_s = 9.2 \times 10^{11} \text{ cm}^{-2}$ and mobility of $\mu = 1.9 \times 10^6 \text{ cm}^2/\text{Vs}$ [25]. The electronic system has a bilayer configuration with symmetric and antisymmetric wave functions for the two lowest subbands and subband separation of $\Delta_{SAS} = 1.4 \text{ meV}$. As demonstrated in a previous report [21], such structure is suitable for the present investigation due to the long spin coherence time comparable with $1/f_1$.

Figure 2(a) shows the KR signal as function of B_{ext} plotted for several applied voltages in the $B_{ext} \perp E$ configuration. Unexpectedly, a KR oscillation with field period $\Delta B_{ext} = 12.5$ to 12.8 mT was observed resembling a RSA pattern. By setting $f_1 = 76 \text{ MHz}$, we get an effective $|g| = 0.424$ to 0.434 showing an electrically-tunable precession frequency. We emphasize that there is no additional optical pump beam, and the detection is only lock in f_2 that acts as electrical spin pump. CISP signal was not expected in this $B_{in} \parallel B_{ext}$ geometry, since the in-plane CISP along \hat{y} can not precess around B_{ext} and thus it can not be detected by polar KR because there is no out-of-plane component. The $B_{ext} \parallel E$ configuration is necessary for a direct measurement of the CISP [16] as we also show in Figure 1(b).

The observation of this remarkable characteristic requires a spin component out of the B_{ext} axis, therefore it implies that pulses in the same laser beam play a two-fold role to reorient and detect the CISP. The electron spin coherence generation by a linearly polarized laser was ob-

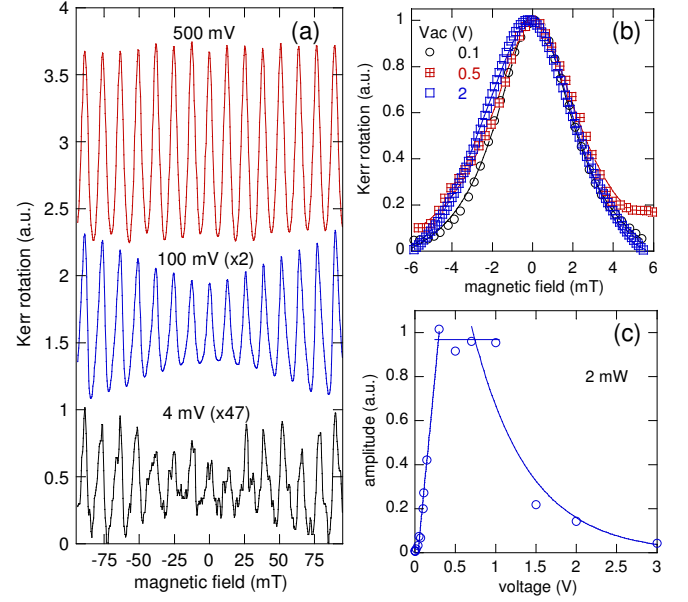


FIG. 2: (Color online) Electrical dependence of the CISP manipulation. (a) B_{ext} scans (scaled for clarity) of the KR signal for different applied voltages. (b) Detail of the normalized zero-field peak with a fitted Lorentzian curve for several voltages. (c) KR amplitude dependence on the external voltage.

served in a previous study [26]. However, the optical reorientation and amplification of the electrically-induced spin polarization is completely unexplored.

The RSA pattern in the CISP signal can be explained as follows. The experiment is initiated by the application of an electrical current which induces spin polarization in the in-plane direction along the B_{in} axis. Figure 1(d) shows that component (S_y) which is constant in time and spatially homogeneous. After electrical generation, a linearly polarized laser pulse reorients the current-induced spin polarization to the out-of-plane direction and generates the S_z component. The first pulse arrives at $t=0$ and allows the precession of S_z around the total magnetic field (B_T) (see also Figure 1(d)). A pulse of the same laser beam acts as a probe and detects the CISP oscillations with the KR lock in the current modulation frequency. Due to the long spin coherence time of the electron system, the pulse temporal train structure leads to the amplification of the z component for fields on resonance. In Figure 1(d) diagram, the blue and red curves (solid lines) are the ϕ_K oscillations for successive pulses and the black curves (dashed lines) are the resulting components. This picture agrees with all the presented data in this report.

Another possible explanation could be that signal arises from a purely optical spin generation in a typical RSA with the absorption somehow enhanced in the presence of an electrical current. In that case, the first probe pulse does not reorient the CISP but it creates the spin polarization. This possibility was ruled out by

performing an additional experiment using a circularly or linearly polarized pump beam and sweeping the magnetic field at different fixed pump-probe delays. The detection was locked in the optical pump frequency using a photoelastic modulator. With the application of an electric field, the RSA vanishes due to the drag of the spin packets destroying the amplification condition [27].

Figure 2(a) shows the enhancement of the RSA pattern amplitude by raising the applied voltage (and current) as expected for electrical spin generation [16]. Figure 2(b) displays a comparison of the zero-field peak for three normalized curves at different voltages. The data points were fitted by a Lorentzian curve $\phi_K = A/[(\omega_L \tau_s)^2 + 1]$ with half-width $B_{1/2} = \hbar/(g\mu_B \tau_s)$ where A is the KR amplitude, $\omega_L = g\mu_B B_{ext}/\hbar$ is the Larmor frequency with the electron g-factor g , Bohr magneton μ_B , Planck's constant \hbar , and τ_s is the spin lifetime. In the studied voltage range, the lineshape does not change significantly implying in an approximately constant $\tau_s = 8$ to 10 ns [27]. The results for the fitted amplitude are plotted in Figure 2(c) showing a lever arm of 0.37 between the KR amplitude gain and the applied voltage increment. This linear gain reaches saturation at 0.5 V and reverts to an exponential decay for voltages above 1 V possibly due to current heating. The temperature dependence will be discussed below.

As depicted in Figure 2 for the voltage dependence, the optical power influence is shown in Figure 3. Figure 3(a) displays the lineshape change from broad complex structures to single Lorentzian curves. The unusual RSA profile for low power corresponds to the signal at trion resonance [15] indicating a strong interdependence of electron and hole dynamics. The increasing RSA amplitude with increasing field for low power implies that faster electron spin precession enhances spin polarization (see also figure 2(a)). Such feature was associated with long hole spin relaxation compared to trion recombination (for example, ten times larger) [15]. Both high current and optical power appear to reduce that ratio which leads to a constant amplitude for increasing B_{ext} . The zero-field lineshape with the increasing optical power is plotted in Figure 3(b) and the fitting results for the amplitude and τ_s are shown in Figure 3(c). The amplitude increases linearly with the optical power as obtained for the voltage parameter but, in contrast, there is a strong reduction of spin lifetime with high power. In pump-probe experiments [10], the decreasing of τ_s at high pump density was associated with the electrons delocalization caused by their heating due to the interaction with the photogenerated carriers.

Figure 4 displays the signal dependence over an extended range of B_{ext} , temperature and position in a Hall bar device. In Figure 4(a), the signal shows a build-up from zero to 0.75 T followed by a slow oscillation with approximate period of 8 T. For the common all-optical RSA, the amplification effect vanishes typically for mod-

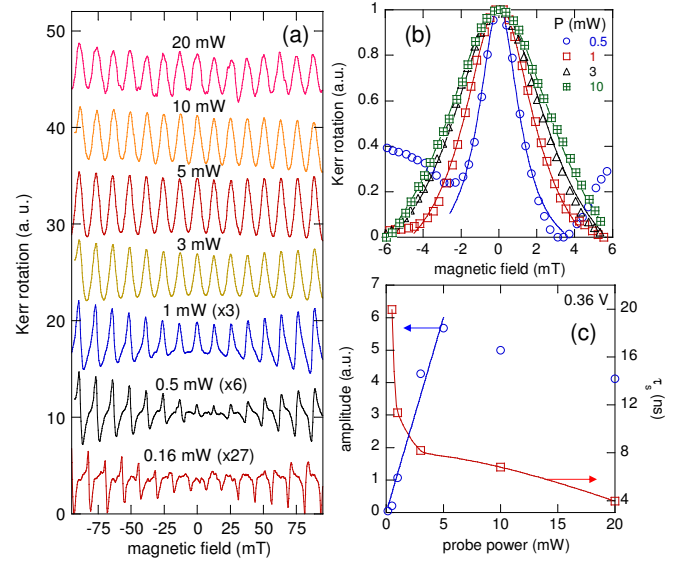


FIG. 3: (Color online) Power dependence of the CISP control. (a) B_{ext} scans of the KR signal for different optical power. The curves were scaled for clarity. (b) Detail of the normalized data fit for different power. (c) KR amplitude and spin lifetime dependence for the zero-field peak.

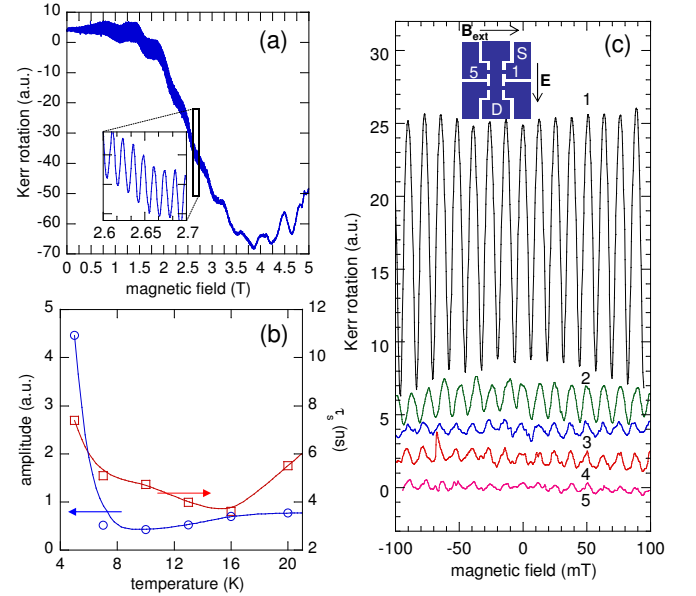


FIG. 4: (Color online) CISP optical amplification dependence on (a) magnetic field, (b) temperature, and (c) position relative to the current source and drain contacts.

erate magnetic field (0.5 to 2 T) [3, 6, 15] due to the spread in the ensemble g factors which results in an inhomogeneous dephasing. In the present approach, the RSA pattern in figure 4(a) holds a constant amplitude up to 3 T and it is strongly suppressed only around 4.25 T. The slow oscillation is associated with the time delay between optical reorientation pump and probe. The measured field period corresponds to $\Delta t = 20$ ps which

is similar to the trion recombination lifetime [28].

The relevance of current heating, as indicated in figures 2(c) and 3(c) decays, was studied by directly raising the temperature up to 20 K. Although the electron spin lifetime slowly oscillates between 4 and 8 ns, a remarkably strong dependence drops the signal amplitude to about 20% above 5 K. This observation may be explained by a similar temperature dependence measured for the hole spin relaxation time and related to the spin-orbit coupling for localized holes [15]. Therefore, the hole spin is a relevant figure in the optical manipulation of the CIPS with dominant contribution in the formation of the trion complex and the resulting electron spin polarization.

An asymmetric current flow was produced in the Hall bar device in order to test the spatial dependence of the CISP amplification. Figure 4(c) shows the signal measured at five different positions. The current flows from the source contact (S) at the right side of the central channel to the drain at channel bottom (D). The signal is stronger when approaching the injection contact (position 1), approximately constant inside the central channel (2 to 4 positions) and much weaker when close to a region with almost no current flow (position 5). Remarkably, the data shows that the spin polarization induced by the current can be directly mapped by the spatial dependence of the optical amplification level.

Having obtained the spin dynamics key parameters, we demonstrate the experimental method capability as sensor of the electrically-tunable internal magnetic field. First, we continue to study the $B_{ext} \perp E$ configuration. Figure 5(a) shows the RSA patterns for several applied voltages where $B_{in} \parallel B_{ext}$. It is visually clear that the zero-field peak is slightly shifted to negative B_{ext} at 1 V due to the addition of a positive B_{in} of 0.55 mT [29]. While the central peak for the other two voltages are well aligned at $B_{ext}=0$, a larger mismatch is shown by the dashed vertical lines at higher external magnetic field strength, for example at -40 mT, as result of a complementary change in the precession frequency. For larger voltages, the manifestation of the spin Hall effect was observed in a large out-of-plane symmetric polarization peak developed together with the RSA oscillation [21].

Finally, we verify the initial assumption of an in-plane CISP in the electron system. To directly measure the spin polarization along \hat{y} , we rotate B_{ext} to the \hat{x} axis as shown in Figure 1(b). The results for the $B_{ext} \parallel E$ configuration are shown in Figure 5(b) and Figure 5(c). The zero-field peak has lower amplitude as expected for an anisotropic relaxation, between the y and z spin components [4, 22], which is electric-field tunable in our experiment. Furthermore, now that B_{in} and B_{ext} are not longer parallel and the CISP can precess around the magnetic field, the KR signal in Figure 5(c) displays an antisymmetric Lorentzian curve which is the signature for the current-induced spin polarization in the \hat{y} direction [16]. As for the previous SHE experiment [21], the RSA pat-

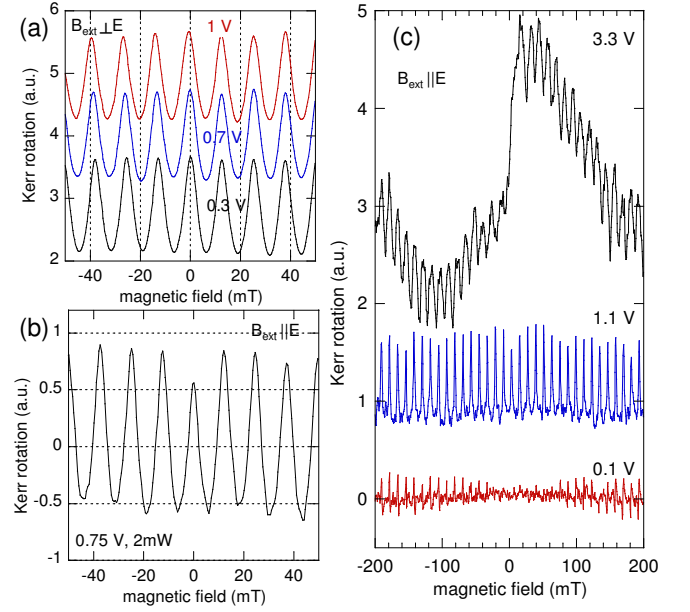


FIG. 5: (Color online) Dependence of the RSA pattern on B_{in} for the configuration: (a) $B_{ext} \perp E$ and (b) $B_{ext} \parallel E$. (c) Direct measurement of the in-plane spin polarization.

tern is still observed and the resonance sharpness change to broad oscillations when the spin packets are dragged by the large electric field.

In summary, we demonstrated the resonant amplification and reorientation of the CISP using a train of optical pulses. We bring together two different approaches, the all-optical RSA and the electrical generation of the spin polarization, making possible the study of the spin polarization components as well as the parameters of the spin dynamics in a single experimental geometry with configuration B_{ext} perpendicular to E . The data dependence on the most relevant parameters was presented. The electron and hole spins displayed an interdependent dynamics where the last is crucial for the effective electron polarization reflected in the oscillations lineshape. The RSA pattern revealed an electrically-tunable internal magnetic field and, for the B_{ext} parallel to E configuration, the signal evolves into a antisymmetric polarization peak at large electrical fields. The application of the reported effect could provide a path for the implementation of spin current sources induced by charge currents and manipulated by optical ways.

A financial support of this work by grants 2009/15007-5, 2010/09880-5, and 2013/03450-7, São Paulo Research Foundation (FAPESP) and CNPq is acknowledged. All measurements were done in the LNMS at DFMT-IFUSP.

* Corresponding author.

Electronic address: felixggh@if.usp.br

- [1] D.D. Awschalom and M.E. Flatté, *Nature Physics* **3**, 153 (2007).
- [2] M.M. Glazov, *Physics of the Solid State* **54**, 1 (2012).
- [3] J.M. Kikkawa and D.D. Awschalom, *Nature* **397**, 139 (1999).
- [4] I.A. Yugova, M.M. Glazov, D.R. Yakovlev, A.A. Sokolova, and M. Bayer, *Phys. Rev. B* **85**, 125304 (2012).
- [5] A. Greulich, D.R. Yakovlev, A. Shabaev, A.L. Efros, I.A. Yugova, R. Oulton, V. Stavarache, D. Reuter, A. Wieck, M. Bayer, *Science* **313**, 341 (2006).
- [6] T. Korn, M. Griesbeck, M. Kugler, S. Furthmeier, C. Gradl, M. Hirmer, D. Schuh, W. Wegscheider, K. Korzekwa, P. Machnikowski, T. Kuhn, M.M. Glazov, E.Ya. Sherman, and C. Schüller, *Proc. of SPIE* **8461**, 84610O (2012).
- [7] M.M. Glazov and E.L. Ivchenko, *Semiconductors* **42**, 951 (2008).
- [8] M. Griesbeck, M.M. Glazov, E.Ya. Sherman, D. Schuh, W. Wegscheider, C. Schüller, and T. Korn, *Phys. Rev. B* **85**, 085313 (2012).
- [9] E.A. Zhukov, O.A. Yugov, I.A. Yugova, D.R. Yakovlev, G. Karczewski, T. Wojtowicz, J. Kossut, and M. Bayer, *Phys. Rev. B* **86**, 245314 (2012).
- [10] E.A. Zhukov, D.R. Yakovlev, M. Bayer, M.M. Glazov, E.L. Ivchenko, G. Karczewski, T. Wojtowicz, and J. Kossut, *Phys. Rev. B* **76**, 205310 (2007).
- [11] K. Korzekwa, C. Gradl, M. Kugler, S. Furthmeier, M. Griesbeck, M. Hirmer, D. Schuh, W. Wegscheider, T. Kuhn, C. Schüller, T. Korn, and P. Machnikowski, *Phys. Rev. B* **88**, 155303 (2013).
- [12] S. Spatzek, S. Varwig, M.M. Glazov, I.A. Yugova, A. Schwan, D.R. Yakovlev, D. Reuter, A.D. Wieck, and M. Bayer, *Phys. Rev. B* **84**, 115309 (2011).
- [13] S. Varwig, A. Schwan, D. Barmascheid, C. Müller, A. Greulich, I.A. Yugova, D.R. Yakovlev, D. Reuter, A.D. Wieck, and M. Bayer, *Phys. Rev. B* **86**, 075321 (2012).
- [14] F. Fras, B. Eble, B. Siarry, F. Bernardot, A. Miard, A. Lemaître, C. Testelin, and M. Chamarro, *Phys. Rev. B* **86**, 161303(R) (2012).
- [15] I.A. Yugova, A.A. Sokolova, D.R. Yakovlev, A. Greulich, D. Reuter, A.D. Wieck, and M. Bayer, *Phys. Rev. Lett.* **102**, 167402 (2009).
- [16] Y.K. Kato, R.C. Myers, A.C. Gossard, and D.D. Awschalom, *Phys. Rev. Lett.* **93**, 176601 (2004).
- [17] I. Stepanov, S. Kuhlen, M. Ersfeld, M. Lepsa, and B. Beschoten, *Appl. Phys. Lett.* **104**, 062406 (2014).
- [18] L. Meier, G. Salis, E. Gini, I. Shorubalko, and K. Ensslin, *Phys. Rev. B* **77**, 035305 (2008).
- [19] V. Sih and D.D. Awschalom, *J. Appl. Phys.* **101**, 081710 (2007).
- [20] V. Sih, R.C. Myers, Y.K. Kato, W.H. Lau, A.C. Gossard, and D.D. Awschalom, *Nature Physics* **1**, 31 (2005).
- [21] F.G.G. Hernandez, L.M. Nunes, G.M. Gusev, and A.K. Bakarov, *Phys. Rev. B* **88**, 161305(R) (2013).
- [22] Y. Kato, R.C. Myers, A.C. Gossard, and D.D. Awschalom, *Nature* **427**, 50 (2003).
- [23] J.M. Kikkawa and D.D. Awschalom, *Nature* **397**, 139 (1999).
- [24] S. Kuhlen, K. Schmalbuch, M. Hagedorn, P. Schlammes, M. Patt, M. Lepsa, G. Güntherodt, and B. Beschoten, *Phys. Rev. Lett.* **109**, 146603 (2012).
- [25] The high mobility of the sample limits the voltage application in the channel to less than 10% of the supplied voltage at the contacts with the current in the order of a few mA.
- [26] K. Schmalbuch, S. Göbbels, Ph. Schäfers, Ch. Rodenbücher, P. Schlammes, Th. Schäpers, M. Lepsa, G. Güntherodt, and B. Beschoten, *Phys. Rev. Lett.* **105**, 246603 (2010).
- [27] See Supplemental Material for complementary data on the resonant spin amplification.
- [28] D.R. Yakovlev and M. Bayer, *Spin Physics in Semiconductors*, Chapter 6, edited by M.I. Dyakonov (Springer, Berlin, 2008).
- [29] The full voltage range characterization of B_{in} was reported by us in reference [21].